Cell Reports, Volume *36*

Supplemental information

CXCL10^{+} peripheral activation niches couple preferred sites of Th1 entry with optimal APC encounter

Hen Prizant, Nilesh Patil, Seble Negatu, Noor Bala, Alexander McGurk, Scott A. Leddon, Angela Hughson, Tristan D. McRae, Yu-Rong Gao, Alexandra M. Livingstone, Joanna R. Groom, Andrew D. Luster, and Deborah J. Fowell

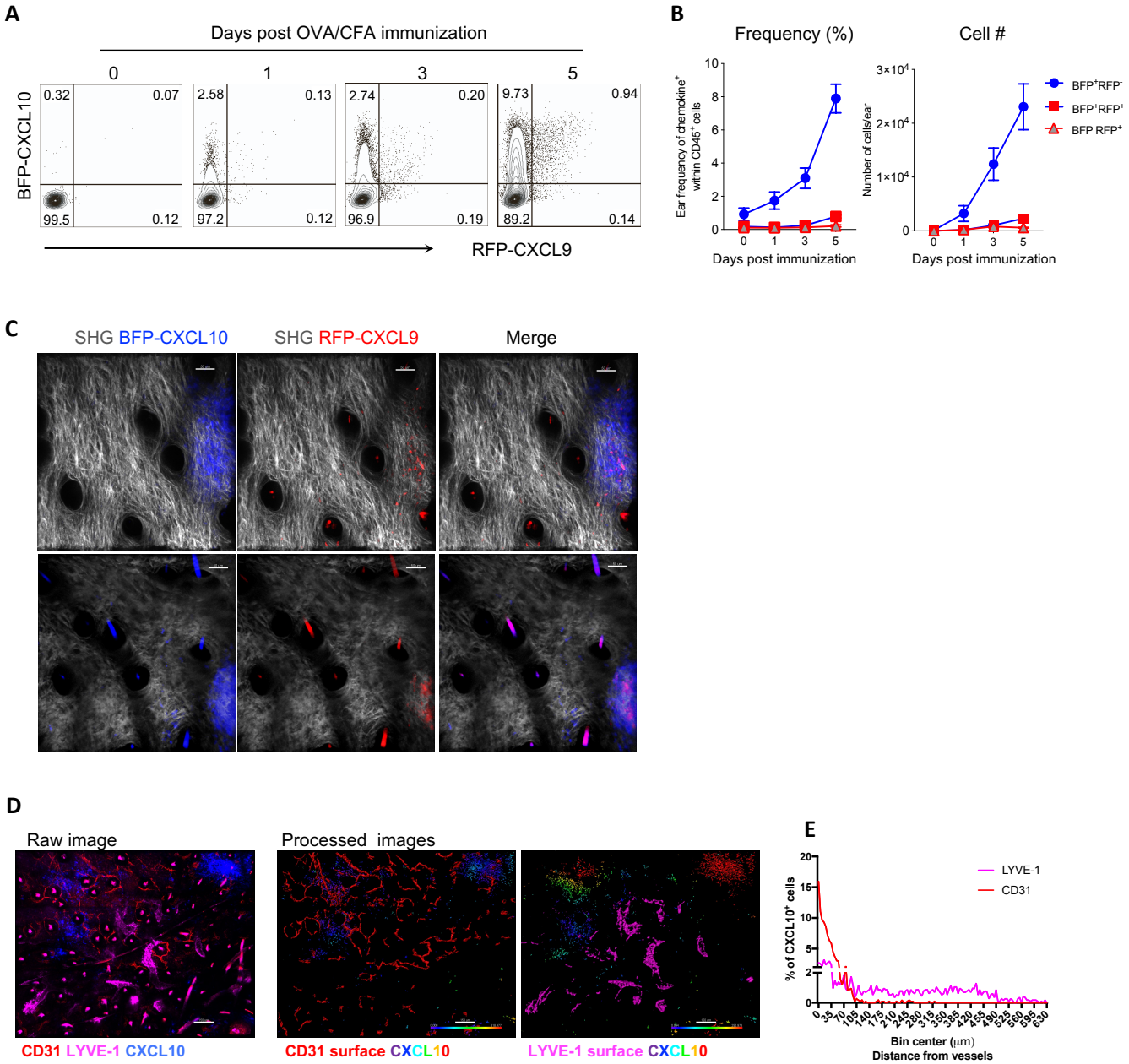

Figure S1. CXCR3 chemokine expression and distribution within the inflamed skin
REX3 mice immunized with OVA/CFA in the ear dermis. **(A)** Representative plots and quantification **(B)** of frequency (left) and number (right) of BFP-CXCL10 and RFP-CXCL9 expressing cells within live singlets CD45⁺ cells, by flow cytometry. **(C)** Two representative chemokine-rich clusters with colocalization of BFP-CXCL10⁺ cells with RFP-CXCL9⁺ cells. Scale bar, 50 μm. **(D)** Representative IV-MPM tiled image and **(E)** quantification of BFP-CXCL10⁺ cells distance from CD31⁺ and LYVE-1⁺ vessels within the same representative imaging volume. Scale bar, 100 μm. Anti-CD31 and anti-LYVE-1 antibodies co-injected i.d. to the ear 2 hours prior to imaging. Related to Figure 1.

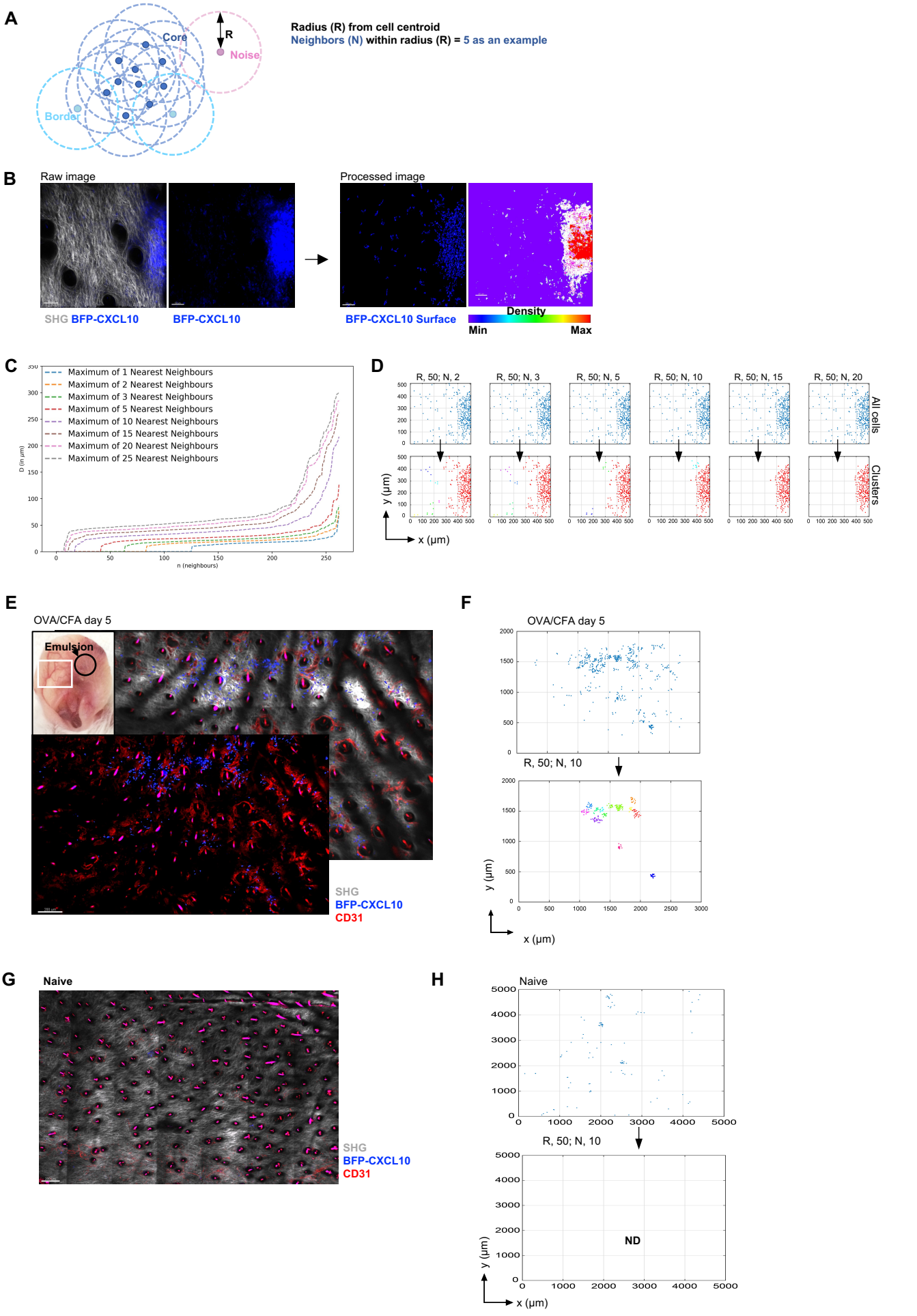

Figure S2. Selecting criteria for BFP-CXCL10⁺ cell clustering

Figure S2. Selecting criteria for BFP-CXCL10^{+} cell clustering

DBSCAN-based machine learning algorithm was developed to unbiasedly and semi-automatically define cell clusters in 3D across different inflamed ears and conditions, using Python. **(A)** Clusters were defined as regions of high density. Each BFP-CXCL10^{+} cells was reconstructed, rendered and registered as a point in space using Imaris and Python. A point (cell centroid) was designated a given radius, R (μm). Each point was defined as a core point within the cluster if it had at least a specified number of neighbor points (N) within its specified radius (R). A point was defined a boarder point if it had fewer than N points within R, but had at least one core point in its radius. A noise point was any point that was not a core point nor a border point, and therefore not part of a cluster. **(B)** BFP-CXCL10^{+} cell cluster (blue) within the d5 OVA/CFA immunized REX3 dermis, by IV-MPM: gray, SHG; scale bar, 50μm. In processed image, BFP-CXCL10^{+} cells were reconstructed and volumetrically rendered along with a cluster surface rendering in 3D using Imaris. **(C)** Combinations of different R and N were plotted using a grid-search approach to find inflection points after which return on metric of choice is incremental. **(D)** Visual examples of different N cutoffs with R=50 μm, using DBSCAN-based algorithm in Python. **(E)** BFP-CXCL10^{+} cell clusters (blue) within d5 OVA/CFA immunized REX3 dermis, tiled image composed of 18 imaging fields of 500 (x) x 500 (y) x 60 (z) μm by IV-MPM: CD31^{+} vessels, red; tiled image scale bar, 200μm. **(F)** DBSCAN-based algorithm was used for 3D cluster identification (multi-color) and reconstruction, using Python; R=50 μm, N=10. **(G)** BFP-CXCL10^{+} cells (blue) within a naïve REX3 dermis, tiled image composed of 18 imaging fields as in E. **(H)** DBSCAN-based algorithm was used for 3D cluster identification and reconstruction, using Python; R=50 μm, N=10. Related to Figures 1, 3 and 5.

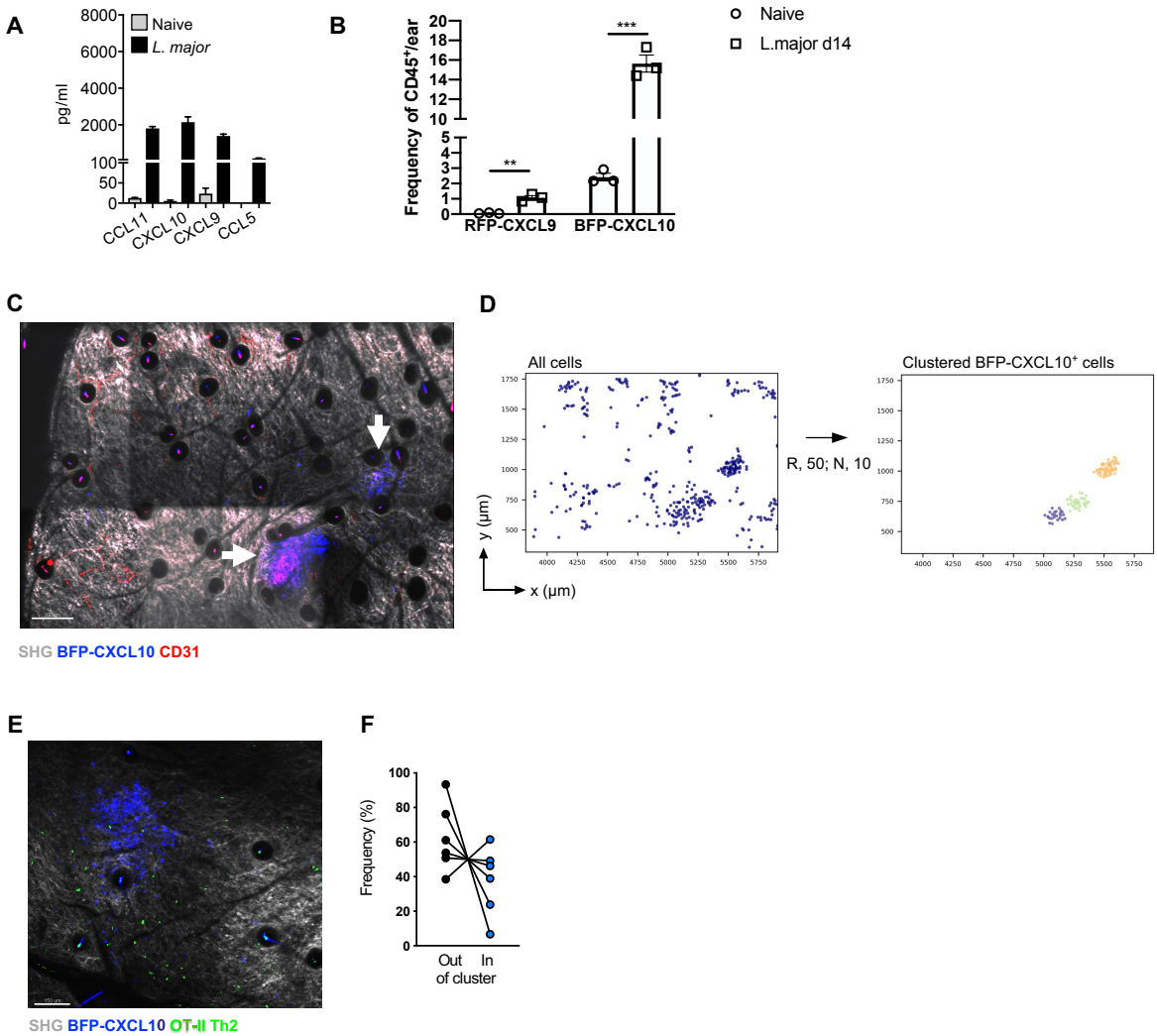

Figure S3. CXCL10⁺ cell clustering in the *L. major* infected skin and lack of spatial preference for Th2 cells.

(A) Chemokine protein levels from naïve and 14-day *L. major* infected WT ears, by Luminex. **(B)** frequency of BFP-CXCL10 and RFP-CXCL9 expressing cells within live singlets CD45⁺ cells from 14 day *L. major* infected REX3 ears, by flow cytometry. **(C)** Perivascular clustering of BFP-CXCL10⁺ cells (blue) within 14-day *L. major* infected REX3 dermis, by IV-MPM: scale bar, 200 µm; gray, SHG; anti-CD31 (red) antibody injected i.v. 15 minutes before imaging. **(D)** Cluster analysis using DBSCAN-based algorithm. **A-D** Related to Figure 1. **(E)** Adoptively transferred fluorescently labeled OT-II Th2 cell (green) localization to BFP-CXCL10⁺ clusters (blue) within d5 OVA/CFA immunized REX3 ear. Maximal z-projection image by IV-MPM: scale bar, 50µm. **(F)** Percentage of OT-II Th2 cells inside or outside of BFP-CXCL10⁺ clusters in d5 OVA/CFA immunized REX3 dermis, by IV-MPM and Imaris. Pooled data from 3 independent experiments, 6 ears, 12 imaging volumes. **E-F** Related to Figure 2.

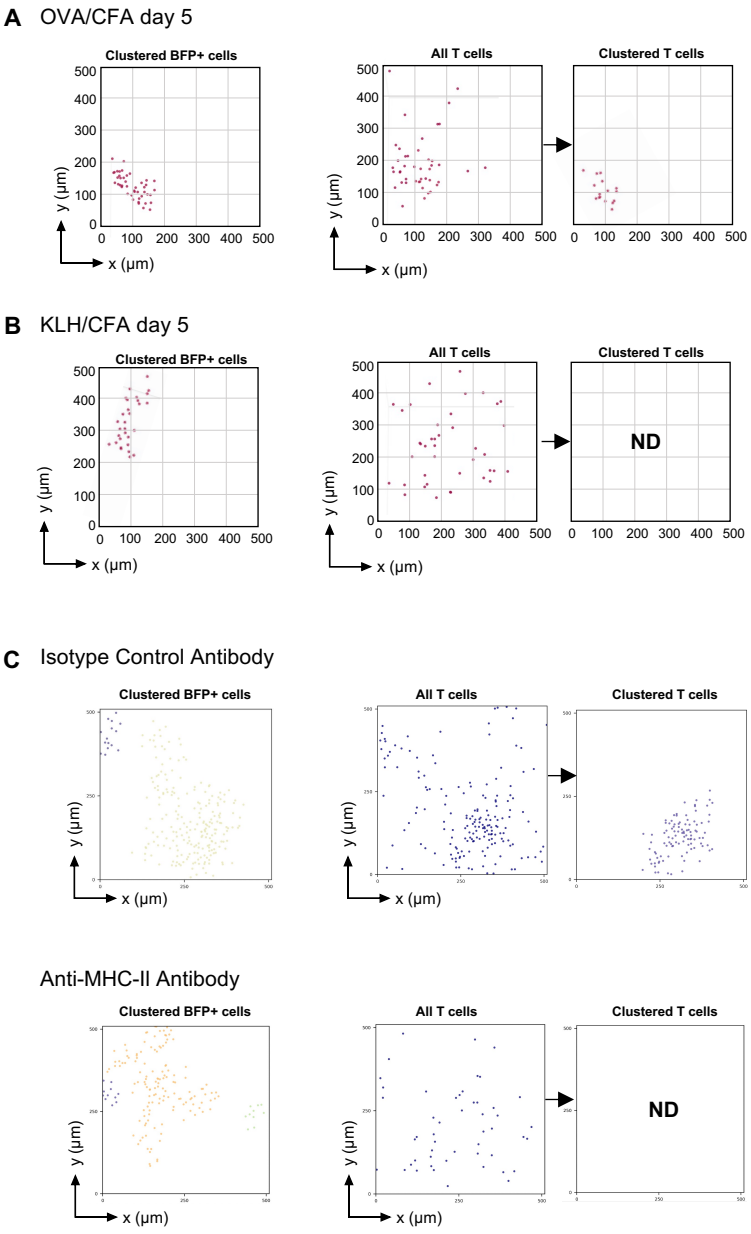

Figure S4. Antigen-dependent Th1 accumulation in BFP-CXCL10⁺ clusters
Adoptively transferred fluorescently labeled OT-II WT Th1 cell localization to BFP-CXCL10⁺ clusters within d5 OVA/CFA and KLH/CFA immunized REX3 ear identified by multiphoton microscopy. **(A, B)** DBSCAN-based algorithm for semi-automated 3D cluster reconstruction of BFP-CXCL10⁺ (left) and Th1 cells (right) from OVA/CFA **(A)** and KLH/CFA **(B)** immunized REX3 ears. ND, none detected. Representative analysis of images shown in Fig. 2D. **(C)** Th1 transfers and immunization with OVA/CFA were performed as in (**A, B**). Six hours prior to imaging, isotype control or anti-MHC-II Ab was administered i.d. in the d5 immunized ear. Multiphoton images were analyzed using the DBSCAN-based algorithm for semi-automated 3D cluster reconstruction of BFP+ cells and transferred Th1 cells. Related to Figure 2.

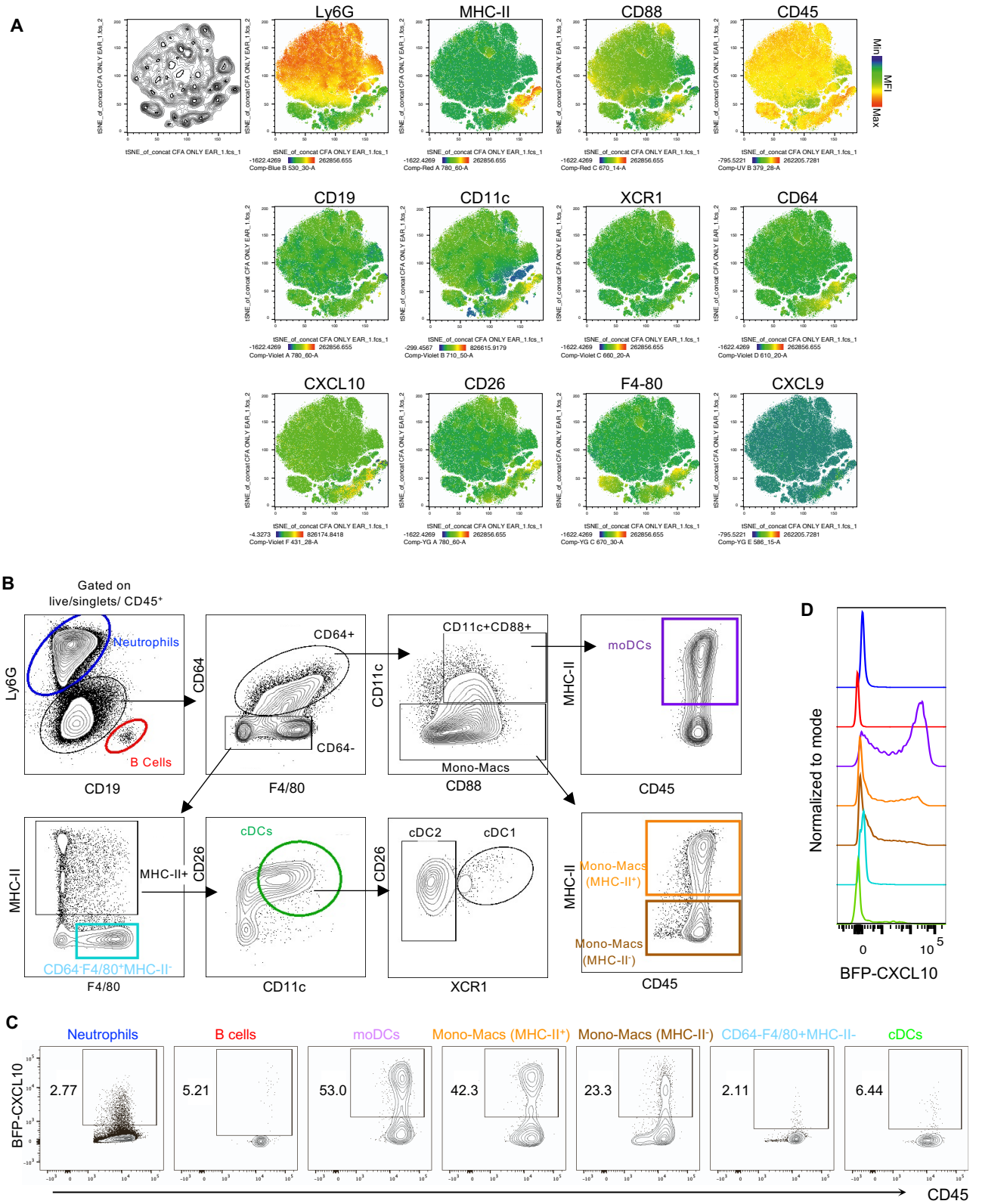

Figure S5. Gating strategies to define the immune subsets with the inflamed skin

(A) tSNE analysis was performed on singlet live CD45$^+$ cells using concatenated multi-color flow cytometry data from d5 OVA/CFA immunized REX3 ears. **(B)** Gating strategy to define the immune subsets within the immunized skin, pre-gated on singlet live CD45$^+$ cells: Neutrophils, Ly6G^{high}; B cells, CD19$^+$; moDCs, Ly6G^{low}CD19$^-$CD64$^+$F4/80$^+$CD11c$^+$MHC-II$^+$; Mono-Macs (MHC-II$^+$), Ly6G^{low}CD19$^-$CD64$^+$F4/80$^+$CD11c$^-$MHC-II$^+$; Mono-Macs (MHC-II$^-$), Ly6G^{low}CD19$^-$CD64$^+$F4/80$^+$CD11c$^-$MHC-II$^-$; CD64$^-$F4/80$^+$ MHC-II$^-$, Ly6G^{low}CD19$^-$CD64$^-$F4/80$^+$MHC-II$^-$; cDCs, Ly6G^{low}CD19$^-$CD64$^-$F4/80$^{+/-}$MHC-II$^+$CD11c$^+$CD26$^+$; cDC1, CD26$^+$XCR1$^+$; cDC2, CD26$^+$XCR1$^-$. **(C)** Representative plots of BFP-CXCL10 expressing cells within each subset in (B), d5 OVA/CFA immunized REX3 ears. **(D)** Histograms of BFP-CXCL10 expression by subset. Related to Figure 4.

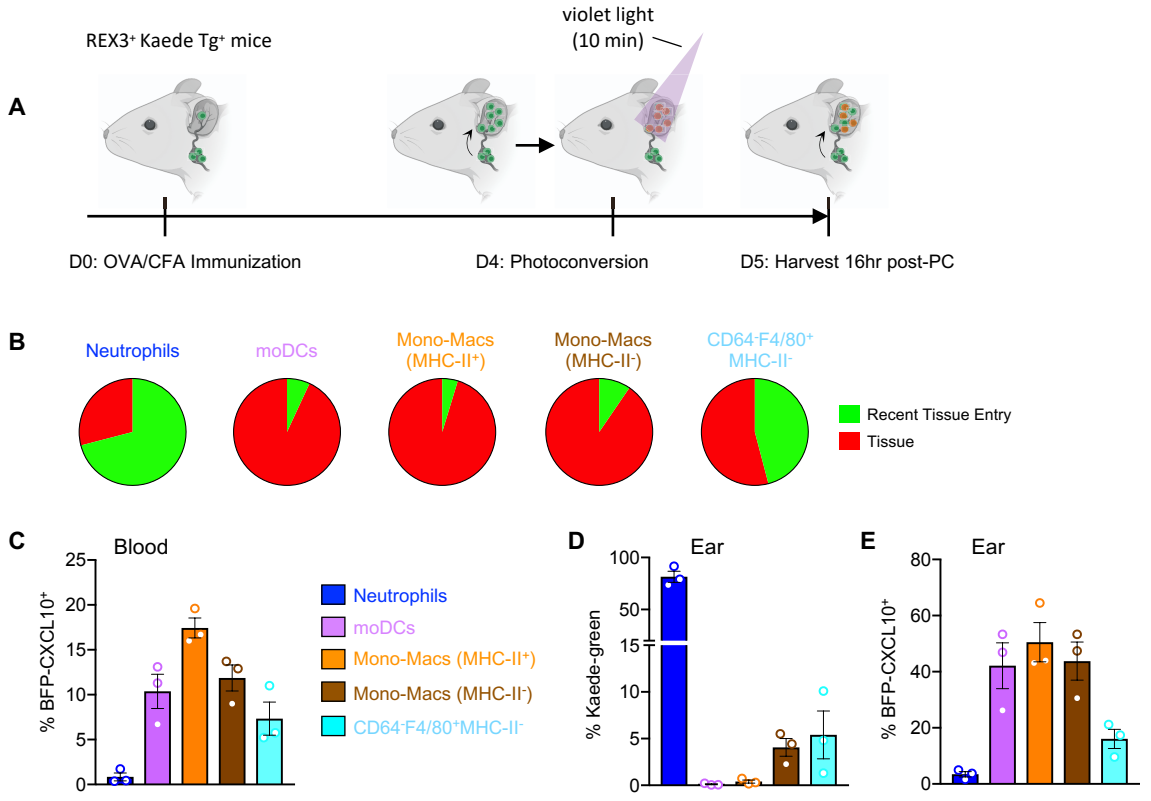

Figure S6. BFP-CXCL10⁺ monocyte and macrophage populations entering the tissue from the blood. (A) REX3⁺ Kaede Tg+ mice were immunized in the ear pinna with OVA/CFA. Day 4, all Kaede-green cells in the inflamed ear were photoconverted to Kaede-red (98% Kaede-red). 16 hours later the ear tissue and blood were harvested for flow cytometry of innate immune subsets, Kaede red/green and BFP-CXCL10 expression: Kaede-red = tissue cells, Kaede-green = cells entering the tissue from the blood in the 16 hours post photo-conversion. Images created with BioRender.com. **(B)** Proportion of Kaede-red and Kaede-green cells within each innate cell subset from the inflamed ear. **(C)** Frequency of BFP-CXCL10⁺ cells within innate subsets in the blood. All blood cells were Kaede-green. **(D)** Frequency of Kaede-green cells entering the tissue from circulation in the 16 hours period from photo-conversion. **(E)** Frequency of BFP-CXCL10⁺ cells within the Kaede-green cells entering the tissue from circulation in the 16 hours period from photo-conversion. One representative experiment of 2 independent experiments, 3-4 mice per group. Related to Figure 4.

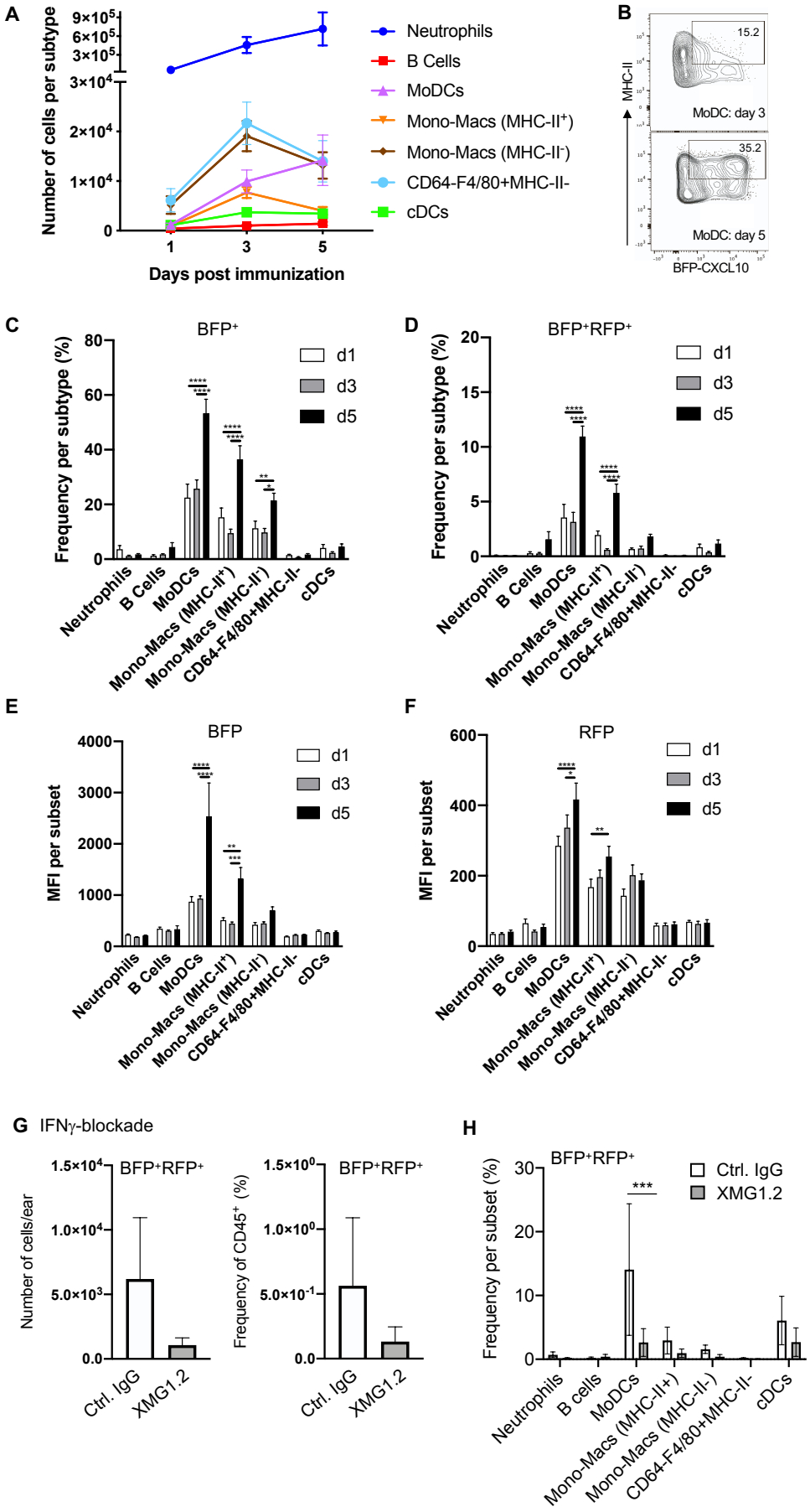

Figure S7. Kinetic analysis of immune subsets and CXCR3 chemokine expression within the immunized skin.

Figure S7. Kinetic analysis of immune subsets and CXCR3 chemokine expression within the immunized skin. **(A)** Number of cells per immune subset within live singlets $CD45^+$ cells from OVA/CFA immunized REX3 ears over time. **(B)** BFP-CXCL10 and MHC-II expression within the moDC population (Ly6GlowCD64+F4/80+Cd11c+MHC-II+) in the ear skin of day 3 and day 5 OVA/CFA immunized REX3 mice. **(C)** Frequency of BFP-$CXCL10^+$ cells and **(D)** BFP-$CXCL10^+$RFP-$CXCL9^+$ cells within each subtype from (B). **(E)** BFP-CXCL10 and **(F)** RFP-CXCL9 MFI within each immune subset from (B). Bars represent mean + SEM. Statistics by two-way ANOVA, *p≤0.05, **p≤0.01, ***p≤0.001, ****p≤0.0001. **(G) (H)** Number and frequency of BFP^+RFP^+ cells in the OVA/CFA immunized REX3 ears following anti-IFNγ blockade (no Th1 transfer). 0.5mg anti-IFNγ Ab (XMG1.2) or control IgG was administered 1 day prior to immunization, the day of immunization (d0) and then daily (d1-d4). Statistics by two-way ANOVA, ***p≤0.001. Related to Figure 7.